Available online at www.sciencedirect.com
ScienceDirect
Energy Reports 8 (2022) 66–74
www.elsevier.com/locate/egyr

2021 6th International Conference on Clean Energy and Power Generation Technology (CEPGT 2021), September 10–12, 2021, Shanghai, China

Performance analysis of a rotating detonation model for future thermal power system using hydrogen as fuel

Mengmeng Zhao[a,b], Linqing Zhang[c,d,*], Weiye Huo[a,b], Hongyu Yang[a,b], Yixiang Yuan[e,f,**]

[a] North China Institute of Aerospace Engineering, Langfang, 065000, China
[b] Hebei Key laboratory of Trans-media Aerial Underwater Vehicle, Langfang, 065000, China
[c] School of Energy Science and Engineering, Harbin Institute of Technology, 150001, Heilongjiang, China
[d] The 41st Institute of the Sixth Academy of Aerosapce Science & Industry Corp, China
[e] Institute of Engineering Thermophysics, Chinese Academy of Sciences, Beijing 100190, China
[f] University of the Chinese Academy of Sciences, Beijing 100049, China

Received 19 October 2021; accepted 2 November 2021
Available online 26 November 2021

Abstract

The thermodynamic cycles of the detonation combustion could potentially deliver a performance increase of 20% beyond the conventional deflagration combustor such as gas turbines and ramjets, thus the detonative combustor is a prospective technology for high-efficiency distributed energy or power systems in the future. Therefore, the core process of rotating detonation combustion using hydrogen as a clean fuel was studied in this paper. A rotating combustor integrated with a supersonic inlet, an isolator, and a nozzle was targeted for the overall performance evaluation using a loose coupling method.

To explore the overall performance of a rotating detonation engine (RDE) combustion model, the study proceeds via three main steps. (1) An axisymmetric semi-isentropic inlet is proposed for the RDE combustor model. The inlet consists of a leading-edge cone and an isentropic outward-turning compression surface. The method for quick design of the external-compression surface was developed and has been verified by the comparison of MOC analysis results with those of computational flow dynamics (CFD) simulations. (2) The combustible mixture gas, produced by the subsonic exiting flow of the isolator mixed with the injected hydrogen, is fed to the annular combustor around which a rotating detonation wave propagates. (3) The rotating detonation simulation for an 'unwrapped' annular combustor was performed and a stable moving detonation wave was achieved with the typical RDE flow-field pattern. The high efficiency of the RDE combustion mode has been demonstrated by the estimated fuel-based specific impulse of 5268 s. The loose coupling method for RDE's performance prediction has been verified by the comparison of the calculated specific impulse with theoretical results published in open literature.

Peer-review under responsibility of the scientific committee of the 6th International Conference on Clean Energy and Power Generation Technology, CEPGT, 2021.

Keywords: Combustion; Rotating detonation; Hydrogen; Computational fluid dynamics

* Corresponding author at: School of Energy Science and Engineering, Harbin Institute of Technology, 150001, Heilongjiang, China.
** Corresponding author at: Institute of Engineering Thermophysics, Chinese Academy of Sciences, Beijing 100190, China.
E-mail addresses: mengezhao@gmail.com (M. Zhao), coordinate_1@163.com (L. Zhang), yuanyx@iet.cn (Y. Yuan).

https://doi.org/10.1016/j.egyr.2021.11.036

Peer-review under responsibility of the scientific committee of the 6th International Conference on Clean Energy and Power Generation Technology, CEPGT, 2021.

1. Introduction

Generally speaking, the widely used gas turbine power generation system is based on the Brayton cycle in the mode of deflagration, and it is difficult to further improve its cycle thermal efficiency. The possibility of improving the thermodynamic cycle by the application of detonative combustion, instead of deflagration, has been studied intensively [1]. Analyzes show that detonation-mode engines can have a theoretical thermodynamic cycle efficiency of more than 20% higher than conventional, deflagration-mode combustion engines [2]. The cycle based on detonation combustion might be a prospective technology for future high-efficiency distributed energy and power systems. A numerical tool was developed for modeling gas turbines equipped with rotating detonation combustors [3]. The deflagration combustion wave propagates with subsonic velocity in the range of cm/s for laminar flames and m/s for turbulent flames, typically, and results in a decrease in pressure and density in the final product mixture. In the case of detonation, the strong combustion wave can propagate at a sonic velocity of km/s, which is sustained by the energy released during the shock-induced premixed combustion and results in increased pressure and density for the final product in contrast to the initial conditions. Thus, the application of different modes of combustion on a thermodynamic cycle can lead to different performances. Fig. 1 shows the comparison of ideal thermodynamic cycles for different combustion processes, where the detonation combustion cycle obtains the highest efficiency with higher temperature and pressure with lower entropy [1].

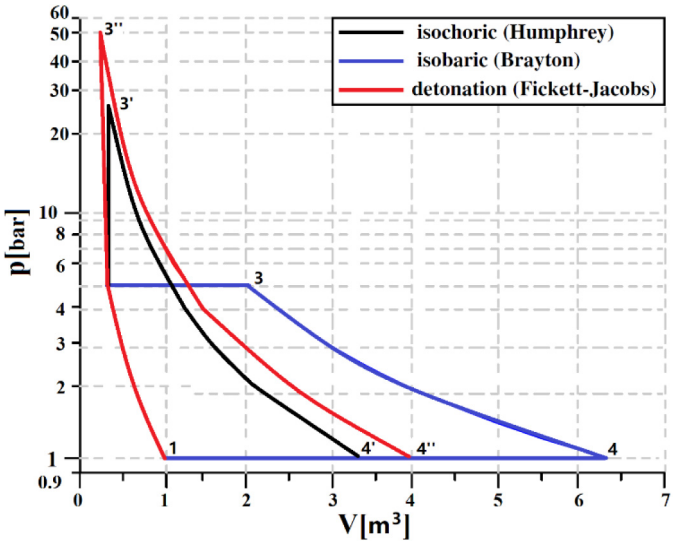

Fig. 1. Thermodynamic Brayton–Joule, Humphrey, and Fickett–Jacobs cycles.

Rotating detonation engines have attracted attention in recent years due to their extremely rapid, detonative combustion with improved theoretical thermal efficiency [4]. The RDE cycle consists of the self-sustained detonation waves continuously rotating around an annular combustor with the continuous incoming fresh reactant mixtures [5]. The annular shape of the RDE combustor also offers ease of integration with the typical axisymmetric engine shape. Simplified engine structures might also be possible through the development of RDEs, resulting in further enhancement of the thrust-to-weight ratio and making it a promising engine technology for future propulsion systems. Parametric studies based on the mathematical modeling of rotating detonation waves equipped with an inlet have been reported [6,7]. The potential advantages of applying rotating detonation to ramjet engines, as sketched in Fig. 2, have been analyzed theatrically in previous reports [1,8]. Unlike the rocket-type RDE, the detonation shock will introduce oblique shock waves propagating upstream and downstream of the detonative reaction front within the RDE ramjet. The thrust is produced when the product gas exhausts out through the nozzle.

The axisymmetric inlet was chosen for this study due to its geometrical compatibility with the annular combustor of the RDE engine with some advantages, such as simple structure, high usage of the windward area, ease of manufacture, ease of storage, and launch [9]. The isentropic compression surface is used for the inlet to reduce the total pressure loss. The method of characteristics (MOC) is employed for this isentropic compression surface

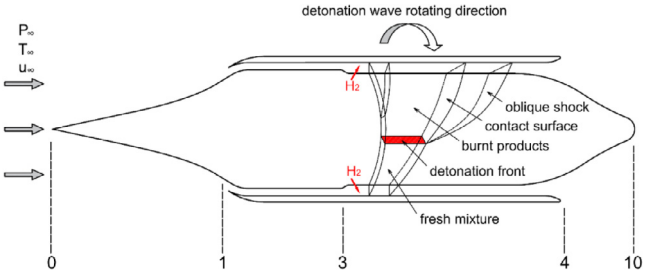

Fig. 2. Schematic illustration of a rotating detonation combustion model. Reference station: 0. Freestream flow; 1. External compression ends (Isolator entry); 3. Isolator exit (Combustor entry); 4. Combustor exit; 10. Nozzle exit.

design [10,11]. For ramjet engines, the isolator is an important component to decelerate the inlet exiting flow to subsonic before entering the combustor [12]. The isolator can bring benefits to the RDE ramjet particularly by tolerating the pressure disturbances downstream induced by the rotating detonation wave, which might degrade or unstart the inlet. This paper focused on the modeling of the RDE engine via CFD tools and the overall performance evaluation of the integration of the RDE with an inlet, an isolator, and a nozzle.

2. Inlet design

2.1. Methodology

As the pure isentropic compression surface with an infinitely thin leading edge and no shock loss is impractical due to its lack of structural integrity [10], the semi-isentropic inlet consisting of an axisymmetric isentropic surface and a leading cone was considered to suit the annular RDE combustor, as shown in Fig. 2.

The physical plane solution of the axisymmetric semi-isentropic inlet can be constructed with a specified inflow Mach number, cowl radius, and the half-angle of the leading cone. The flow field for the leading-edge conical can be resolved numerically based on the Taylor–Maccoll equations and oblique shock relations [13]. The conical shock and the radius of the cowl lip will determine the coordinates of the focal point, as shown in Fig. 3, which is the key parameter for MOC calculation. The initial Mach line originating from the ending point of the cone surface is constructed across the flow field to the focal point. The flow parameters along the initial Mach line are known from the conical flow solutions. The following Mach lines that form the compression fan are all focused on the focal point, which corresponds to the local turning angle of the isentropic compressing surface. The computational mesh, as shown in Fig. 3, is constructed and the flow fields of the isentropic compression regions are solved using the MOC as a finite-difference code.

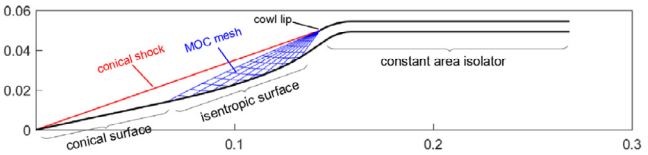

Fig. 3. The characteristic grid used in the design of a semi-isentropic surface for Mach 4 flows. more than half of the lines and the points on the lines have been removed for clarity (dimensions are normalized by cowl radius).

The isolator is generally used to decelerate the incoming flows of ramjet or scramjet before the entrance of the combustor. The additional benefit of the isolator is to tolerate the pressure rise downstream caused by combustion that might degrade or unstart the inlet. A constant-area isolator is used in this paper, as shown in Fig. 3, and the length of the isolator can be estimated by [12]

$$\frac{L}{h} = \frac{\sqrt{\frac{\delta}{h}}}{\sqrt[4]{Re_\delta}} \cdot \frac{\left\{50\left(\frac{p_3}{p_1} - 1\right) + 170\left(\frac{p_3}{p_1} - 1\right)^2\right\}}{M_1^2 - 1} \tag{1}$$

where δ is the boundary-layer momentum thickness at the isolator entrance, h is the height of the annular isolator, and Re_δ is the inlet Reynolds based on the inlet momentum thickness. In practical design, a contracted isolator can be applied for increased compression efficiency to shorten the length of desired exiting flows.

A curved passage is usually needed to turn the deflected flow into the isolator for further deceleration. Fig. 4 illustrates the tuning section which maintains a constant sectional area with a recommended minimum radius of inner body curvature equivalence to four passage heights [10]. With the specified freestream flow conditions (M_0, P_0, T_0), the maximum compression turning angle (θ_{max}), the half-angle of the leading-edge cone (θ_c), and the cowl radius (r), the coded program can generate the inlet profile in the form of coordinates. The flow fields, the exiting flow parameters of the isolator, and the compression efficiency (η) are also resolved. The major parameters for the semi-isentropic inlet calculation are listed in Table 1.

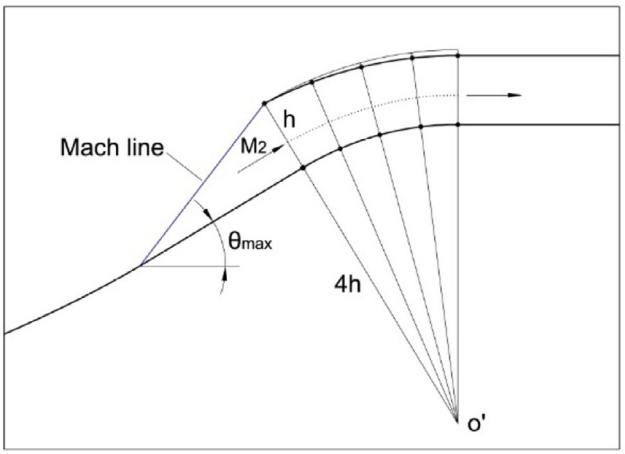

Fig. 4. Turning section connecting compression surface and the isolator.

Table 1. Flow conditions and key parameters for the semi-isentropic inlet.

Input parameters					
M_0	P_0 (kPa)	T_0 (K)	θ_{max}	θ_c	r (m)
4	11.9	216	32°	12°	0.05
Output data					
M2	L/h	h/r	η	M4	
2.44	23.48	0.128	0.52	0.51	

2.2. CFD verification for the inlet design

The verification of the semi-isentropic compression inlet was performed using the CFD code, 'Eilmer4', based on a two-dimensional axisymmetric model. The key parameters for boundary conditions and model geometry definition are listed in Table 1. The computational domain is sketched in Fig. 5 with the view of enlarged details of the grid at the isolator entrance. The non-uniform structured grids cluster toward the wall to capture the detailed flow structures near the boundary layer. A total number of 756,800 cells was selected for CFD computations after a grid study.

The inviscid and compressible model was first employed to validate the external semi-isentropic compression surface for the inlet design using MOC calculation. The simulated results of the Mach number contour, as shown in Fig. 6, indicate that the Mach number of the incoming flow gradually decreases after the conical shock and approaches 2.45 at the isolator entrance. A good agreement between the code program calculated values of 2.44 with CFD simulated values of 2.45 for Mach number at the location of the isolator entrance demonstrates that the code program is sufficient as a preliminary tool for quick design and aerodynamic analysis.

The CFD simulation of the inlet coupled with the isolator was performed using the SST $k-\omega$ turbulence model. The $k-\omega$ model has been shown to be a suitable candidate for supersonic and hypersonic aerothermodynamics

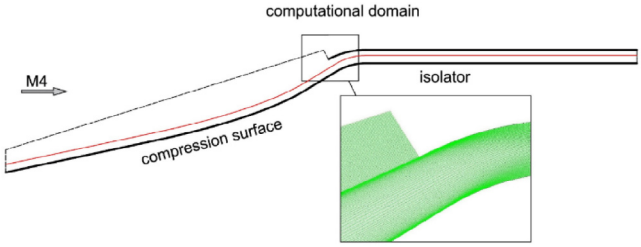

Fig. 5. Computational domain and grid detail near the isolator entrance. The red line at 3.5 mm above the inner body surface is the reference for data extraction of the simulation results. (For interpretation of the references to colour in this figure legend, the reader is referred to the web version of this article.)

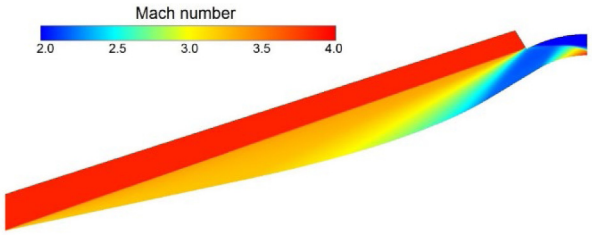

Fig. 6. Mach number contours of CFD simulation results using inviscid flows. Only the external compression portion is displayed for clarity.

numerical applications [14–16]. As for RANS turbulence models without wall function applied to resolve the viscous sublayer, the dimensionless parameter y^+, the normal distance of the first cell from the wall, less than 1 is important for accurate prediction on surface skin friction and heat flux. In the mesh generation for the CFD simulation of the inlet in this paper, the value of y^+ was around 1.0 except in the first few cells from the leading edge where the boundary layer has just started developing. The computed contours of Mach number and static pressure are shown in Figs. 7 and 8, respectively. The effects of viscosity on the lower-momentum flow of the boundary layer and the shock train within the isolator were captured. The deviation of the compression fan away from the focal point arose from the lower-momentum flow of the boundary layer so that the prescribed amount of the incoming flow turning could not take place, resulting in reduced performance of the inlet. The compressed flow was further decelerated to subsonic flow through the shock trains that are triggered at the entrance of the isolator.

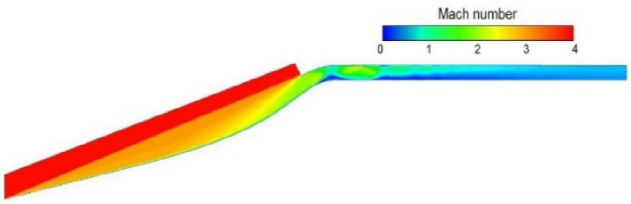

Fig. 7. Mach number contours of CFD simulation results using $k-\omega$ turbulence model.

Mach number and static pressure alone a line at 3.5 mm above the inner body surface was extracted as shown in Fig. 9. The simulated pressure gradually increased till the entrance of the isolator, while a rapid decrease occurred because of the appearance of an expansion at the turning section. The static pressure was further elevated by shock trains and the flow decelerated to subsonic at the isolator exit. The simulated Mach number of 0.66 at the isolator exit is 22% larger than that calculated by the code program. The averaged total pressure at exit is 0.74 MPa, corresponding to the compression efficiency of 0.41 which is lower than the values calculated by the code program.

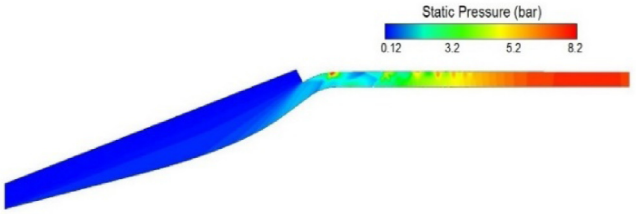

Fig. 8. Static pressure contours of CFD simulation results using $k-\omega$ turbulence model.

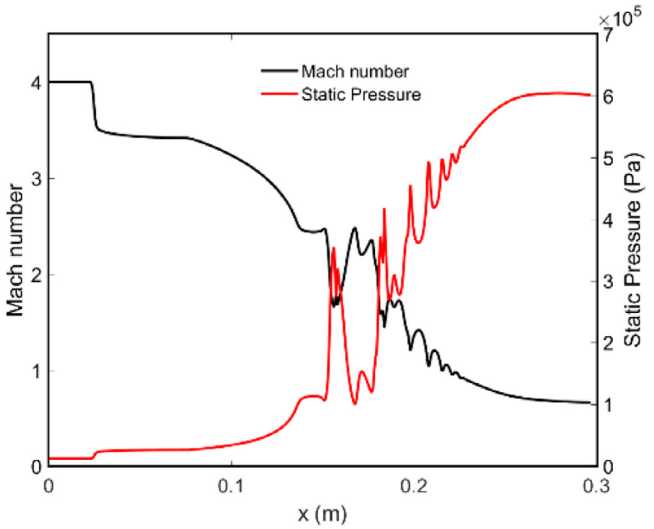

Fig. 9. Mach number and static pressure distributions alone a line at 3.5 mm above the inner body surface.

3. RDE simulation

The isolator exiting flow conditions listed in Table 2 are based on the computational results of the inlet simulations. The hydrogen was chosen as the fuel that is injected through a transverse injector inclined $\theta = 45°$ to the axis at a speed of sonic with a total pressure of 1.5 MPa and a temperature of 300 K. The position of the injector is fixed at the location upstream of the entrance of the annular combustor, as shown in Fig. 1.

The stoichiometric combustible mixture of hydrogen and air was assumed for RED combustion. Constant area mixing was assumed within the control volume (CV), where friction, heat transfer and other losses were neglected. The flow conditions of the mixture were calculated by

$$\dot{m}_{\mathrm{h}} + \dot{m}_3 = \dot{m}_{\mathrm{e}} \tag{2}$$

$$P_3 + \rho_3 u_3^2 + \frac{P_{\mathrm{h}} A_{\mathrm{h}}^* cos\theta}{A} + \frac{\dot{m}_{\mathrm{h}} u_{\mathrm{h}} cos\theta}{A} = P_{\mathrm{e}} + \rho_{\mathrm{e}} u_{\mathrm{e}}^2 \tag{3}$$

$$\dot{m}_{\mathrm{h}} \left(Cp_{\mathrm{h}} T_{\mathrm{h}} + \frac{u_{\mathrm{h}}^2}{2} \right) + \dot{m}_3 \left(Cp_3 T_3 + \frac{u_3^2}{2} \right) = \dot{m}_e \left(Cp_{\mathrm{e}} T_{\mathrm{e}} + \frac{u_{\mathrm{e}}^2}{2} \right) \tag{4}$$

$$\frac{\dot{m}_{\mathrm{h}}}{\dot{m}_3} = 0.0294 \tag{5}$$

in combination with the ideal gas equation of state and the specific heat expression [17]

$$P_{\mathrm{e}} = \rho_{\mathrm{e}} R_{\mathrm{e}} T_{\mathrm{e}} \tag{6}$$

$$\frac{Cp_{\mathrm{e}}}{R_{\mathrm{e}}} = a_1 + a_2 T_{\mathrm{e}} + a_3 T_{\mathrm{e}}^2 + a_4 T_{\mathrm{e}}^3 + a_5 T_{\mathrm{e}}^4 \tag{7}$$

Table 2. Flow conditions of the mixing process.

	Isolator exit	H2 exit	CV exit
P (kPa)	710	790	740
T (K)	880	250	706
u (m/s)	305	1201	366

where subscripts of 3, h and e refer to the flows at the exit of the isolator, hydrogen injection and CV, respectively. R_5 for mixture was obtained based on the mass fraction of air and hydrogen, the values of $a_1 \sim a_5$ can be found in [17]. The conditions of the combustible mixture flow for the rotating detonation simulations are shown in Table 2.

The modeling of the single-wave rotating detonation was performed using Eilmer4 [18] on a High-Performance Computing facility, based on a 2-dimensional 'unwrapped' annular combustor by treating the width of the annulus as having a unit thickness and ignoring curvature and radial effects. To assess the upstream influence of rotating detonation waves on incoming flows, a computation domain (0.325 m $\times$ 0.36 m) consisting of a non-reaction zone and a reaction zone was discretized as a 2-dimensional uniform grid (1300 $\times$ 480 cells) with periodic boundary conditions as shown in Fig. 10(a), which also illustrates the computed contours of temperature at an instant time during a cycle. Note that computational domains are repeated for detonation structural clarity. The transient simulation of viscous compressible flow was carried out with a detailed H_2/O_2 oxidation chemistry mechanism including 8 species (H_2, O_2, H_2O, HO_2, OH, O, H, N_2) and 18 elementary reactions proposed by [19]. The grid sensitivity analysis was performed nominally identical simulations using different mesh densities and confirmed that the mesh resolution with 624,000 elements is sufficient to capture the physically relevant features.

A single-wave detonation was initiated by introducing a small zone (2 mm $\times$ 10 mm) within the reaction zone near the border to the non-reaction zone with a temperature of 2000 K, a pressure of 2.0 MPa, and a velocity of -2000 m/s. Once established, the detonation wave traveled from right to left across the computational domain, as illustrated in Fig. 10(a), simulating a circumferential flight of the wave within the annular combustor. The results illustrate an inclined detonation front with an angle of 78° relative to the wave propagation direction at a rotating speed of 1627 m/s. The C-J detonation wave speed of 1958 m/s estimated by thermodynamic tools [20] is greater than the simulated result of 1663 m/s. The computed pressure and mass fractions for OH throughout the 'unwrapped' annulus at a particular instant in time are shown in Fig. 10(b) and (c). The flow features of the RDE ramjet have been well predicted and labeled in Fig. 10. The distinctive feature of the RDE ramjet compared to most rocket-type RDE is the moving detonation induced compression wave propagating upstream, which can process the incoming airflow and generate a pulse of high pressure in the isolator. The deflagration zone is described clearly in Fig. 10(c) for the OH mass fraction. The products produced by deflagration combustion separate the detonation products from those of the previous cycle. The shear layer vortices appear at the edge of the deflagration product stream. Although a certain amount of fuel is consumed by deflagration, the primary heat release mechanism in an RDE ramjet is detonation.

Assuming isentropic expansion of the detonation products to free-stream static pressure, the fuel-based specific impulse can be estimated based on the computational results of RDE simulations,

$$I_{sp} = \frac{F_g - F_r}{g_0 \dot{m}_{\mathrm{h}}} = \frac{\dot{m}_{10} u_{10} - \dot{m}_1 u_1}{g_0 \dot{m}_h} \tag{8}$$

where the F_g is the gross thrust and F_r is the ram drag. Table 3 compares the calculated specific impulse to that from literature for the hydrogen-fueled RDE model. The high value of the specific impulse demonstrates the RDE as a promising mode for ramjet configurations. Note that the estimated specific impulse here represents the upper limit on the performance we would expect because some of the loss mechanisms in the RDE ramjet operation are neglected.

Table 3. Comparison of fuel-based specific impulse.

	[21]	[22]	Present work
I_{sp} (s)	5383	4860	5068

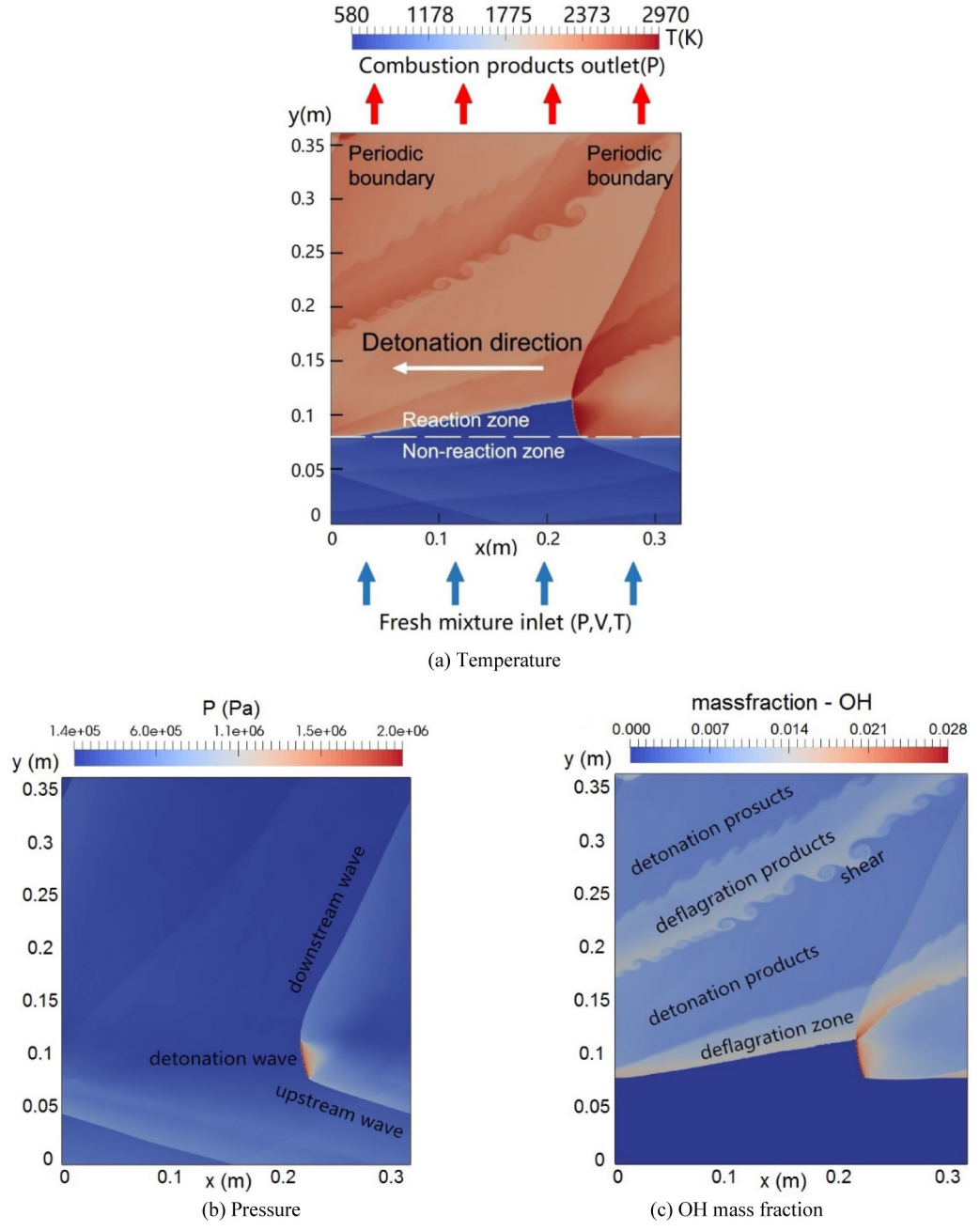

(a) Temperature

(b) Pressure

(c) OH mass fraction

Fig. 10. Computational results within the 'unwrapped' rotating detonation combustor at an instant in time.

4. Conclusion

Considering that the detonative combustion cycle offers a significant increase of thermodynamic efficiency over the conventional power system using a deflagrative combustion mode, this paper focuses on the core process of rotating detonation combustion using hydrogen, which can lay a foundation or provide a reference for its future application in propulsion systems, gas turbines, or other power systems.

The methodology for quick design of the axisymmetric semi-isentropic inlet was proposed and has been verified as a reliable tool by inviscid CFD simulations. The modeling of the inlet coupled with the isolator using $k-\omega$

model indicates that the lower-momentum flows of the boundary layer reduce the performance of the inlet, and the shock trains within the isolator is the major contributor to the total pressure loss. A time-resolved simulation of the combustor was carried out to replicate the actual detonation process and the simulated results were subsequently used to calculate the specific impulse as the known parameters for the nozzle.

Two-dimensional simulations of a hydrogen-fueled rotating detonation model in which the combustor is effectively unfurled and treated as a planar configuration have been achieved. The typical detonation structures and RDE's flow-field pattern have been captured. The calculated thrust of the specific impulse of 5068 s represents a high-efficiency performance compared to conventional deflagrative engines. Based on the comparison of the calculated thrust with theoretical results published in open literature, the loose coupling method proposed in this paper is capable of predicting RDE's performance. Although many efforts have been focused on the research of detonative combustion experimentally and numerically, many crucial problems in all aspects of its systems need to be solved before the effective application of RED on propulsion and power systems in the future.

Declaration of competing interest

The authors declare that they have no known competing financial interests or personal relationships that could have appeared to influence the work reported in this paper.

Acknowledgment

This work was funded by the North China Institute of Aerospace Engineering, NO. GFCJJ202101 and NO. BKY202034.

References

[1] Wolański P. Detonative propulsion. Proc Combust Inst 2013;34(1):125–58.
[2] Kailasanath K. Review of propulsion applications of detonation waves. AIAA J 2000;38(9):1698–708.
[3] Sousa J, Paniagua G, Morata EC. Thermodynamic analysis of a gas turbine engine with a rotating detonation combustor. Vol. 195, 2017, p. 247-56.
[4] Turns SR. An introduction to combustion: Concepts and Applications. 3rd ed.. New York: McGraw-hill; 2012, 3 ed..
[5] Voitsekhovskii B. Stationary spin detonation. Sov J Appl Mech Tech Phys 1960;3(6):157–64.
[6] Braun EM, et al. Airbreathing rotating detonation wave engine cycle analysis. Aerosp Sci Technol 2013;27(1):201–8.
[7] Zhdan S, Bykovskii F, Vedernikov E. Mathematical modeling of a rotating detonation wave in a hydrogen-oxygen mixture. Combust Explos Shock Waves 2007;43(4):449–59.
[8] Lu FK, Braun EM. Rotating detonation wave propulsion: experimental challenges, modeling, and engine concepts. J Propuls Power 2014;30(5):1125–42.
[9] Slater J. Design and analysis tool for external-compression supersonic inlets. In: 50th aiaa aerospace sciences meeting including the new horizons forum and aerospace exposition. 2012.
[10] Mahoney JJ. Inlet for supersonic missiles. AIAA education series, Washington, DC: American Institute of Aeronautics and Astronautics; 1990, p. 1.
[11] Seddon J, Goldsmith E. Intake aerodynamics. American Institute of Aeronautics and Astronautics, Inc; 1999.
[12] Heiser WH, Pratt DT. Hypersonic airbreathing propulsion, Vol. 1. AIAA; 1994.
[13] Anderson JD. Modern compressible flow: with historical perspective, Vol. 12. McGraw-Hill New York; 1990.
[14] Parent B, Sislian JP. Validation of the wilcox k-omega model for flows characteristic to hypersonic airbreathing propulsion. AIAA J 2004;42(2):261–70.
[15] Cutler AD, et al. Supersonic coaxial jet experiment for computational fluid dynamics code validation. AIAA J 2006;44(3):585–92.
[16] Chan W, Jacobs P, Mee D. Suitability of the k–ω turbulence model for scramjet flowfield simulations. Int J Numer Methods Fluids 2012;70(4):493–514.
[17] Burcat A, Ruscic B. Third millenium ideal gas and condensed phase thermochemical database for combustion (with update from active thermochemical tables). Argonne, IL (United States): Argonne National Lab.(ANL); 2005.
[18] Jacobs P, Gollan R. Implementation of a compressible-flow simulation code in the D programming language. In: Applied mechanics and materials. Trans Tech Publ; 2016.
[19] Evans JS, Schexnayder CJ. Influence of chemical kinetics and unmixedness on burning in supersonic hydrogen flames. AIAA J 1980;18(2):188–93.
[20] Gordon S, McBride BJ. Computer program for calculation of complex chemical equilibrium compositions and applications. part 1: analysis. 1994.
[21] Shepherd JE, Kasahara J. Analytical models for the thrust of a rotating detonation engine. 2017.
[22] Schwer D, Kailasanath K. Fluid dynamics of rotating detonation engines with hydrogen and hydrocarbon fuels. Proc Combust Inst 2013;34(2):1991–8.